Cavity Enhanced Immunoassay Measurements in Microtiter Plates using BBCEAS

Zuzana Bajuszova, Zulfiqur Ali, Simon Scott, L. Nitin Seetohul[a], and Meez Islam*

School of Science and Engineering, Teesside University, Borough Road, Middlesbrough, TS1 3BA, United Kingdom

[a]Present address, College of Arts and Science, School of Science & Technology, Nottingham Trent University, Burton Street, Nottingham, NG1 4BU

*To whom correspondence should be addressed. Email: m.islam@tees.ac.uk

We report on the first detailed use of broadband cavity enhanced absorption spectroscopy (BBCEAS) as a detection system for immunoassay. A vertical $R \geq 0.99$ optical cavity was integrated with a motorised XY stage, which functioned as a receptacle for 96 well microtiter plates. The custom built cavity enhanced microplate reader was used to make measurements on a commercially available osteocalcin sandwich ELISA kit. A 30 fold increase in path length was obtained with a minimum detectable change in the absorption coefficient, $\alpha_{min}(t)$, of 5.3×10^{-5} cm^{-1} Hz$^{-1/2}$. This corresponded to a 39 fold increase in the sensitivity of measurement when directly compared to measurements in a conventional microplate reader. Separate measurements of a standard STREP-HRP colorimetric reaction in microtiter plates of differing optical quality produced an increase in sensitivity of up to 115 fold compared to a conventional microplate reader. The sensitivity of the developed setup compared favorably with previous liquid-phase cavity enhanced studies and approaches the sensitivity of typical fluorometric ELISAs. It could benefit any biochemical test which uses single pass absorption as a detection method, through either the label free detection of biologically important molecules at lower concentrations or the reduction in the amount of expensive biochemicals needed for a particular test, leading to cheaper tests.

Enzyme linked Immunosorbent Assays (ELISA) are amongst the most widely used and important bio-analytical techniques currently available. They are based on the detection of highly specific antibody antigen reactions with key characteristics of, accuracy, precision, limit of detection, measurement range, and cost. With the availability of a wide range of disease biomarkers and increased use of expensive reagents an ELISA can be costly to use if several biomarkers need to be measured in an investigation [1]. The most commonly used ELISA detection method involves colorimetric detection through the use of visible wavelength absorption spectroscopy with an appropriate microplate reader. There are, however, a variety of other formats including simple dip strip ELISA [2]. Absorption spectroscopy is simple and widely used but has relatively poor sensitivity when compared to other analytical techniques. This is because the measurement of a small absorption requires the measurement of a small difference between two large signals, corresponding to the intensity with and without sample, unlike for example fluorescence spectroscopy where the measurement can be made in principle against a zero background signal. Consequently, fluorometric detection of ELISA is typically 100 - 1000 times more sensitive than colorimetric detection [3]. However, fluorometric detection requires the fluorescent labeling of some of the ELISA reagents whilst the cost of fluorometric microplate readers is significantly higher than basic

1

colorimetric microplate readers as more expensive optical components are required. Methods which can increase the sensitivity of colorimetric detection are therefore highly desirable as they would potentially allow this simpler, cheaper and label free detection method to be used for tests where currently only fluorometric detection has the required sensitivity.

The Beer–Lambert law states that the absorbance is proportional to the path length of measurement and so the sensitivity of absorption measurements can be improved by increasing the path length. However, increasing the physical path length is not feasible for most bio-analytical applications. Over the past two decades the sensitivity of absorption spectroscopy has been greatly improved through the development of techniques based on the use of optical cavities. These have used high reflectivity dielectric mirrors to form an optical cavity around the sample which allows light entering through the back of one of the mirrors to be essentially multi-passed many times through the sample and thus greatly increase the effective path length of measurement. The first experimental studies were based on cavity ring down spectroscopy (CRDS) [4], which required powerful laser light sources and complex and expensive fast detection equipment to measure the decay in intensity of light exiting the cavity on a microsecond timescale. This 'ring down time' could be directly related to the absorption coefficient of an analyte. Later on an experimentally simpler variant, cavity enhanced absorption spectroscopy (CEAS) [5] was demonstrated. This required only the measurement of the time integrated intensity exiting the cavity and so could use slower and cheaper detection setups but had the disadvantage of requiring calibration measurements to obtain the absorption coefficient of analytes. Further experimental innovations were demonstrated through broadband CEAS (BBCEAS) [6], where a high intensity lamp was used as the light source instead of a laser and coupled with a multiplex detector to allow simultaneous measurement across a wide wavelength range. LED-BBCEAS has additionally reduced complexity and cost through the use of a high intensity LED as the light source [7]. Most of the previous cavity based measurements have been made on gas-phase analytes as low background scattering and absorption by gases allows a very high number of passes ($>10^4$ with suitable high reflectivity mirrors) to be achieved. Only a few liquid-phase cavity based studies have been reported to date as the solvent related scattering and absorption losses are much higher [8]–[14]. However, for bio-analytical applications the majority of analytes are in the liquid-phase. Many of the previous liquid-phase studies have used CRDS and have focused on using CRDS as a detection method for high performance liquid chromatography (HPLC). Recently LED-BBCEAS has been applied to liquid-phase measurements both in cuvettes [15], [16] and also as a detector for HPLC measurements [17]. The sensitivity of these measurements was comparable to the CRDS measurements whilst using a substantially less complex and lower cost experimental setup. There have been no previously reported CEAS studies that have been applied to more complex and practically relevant liquid-phase assays such us immunoassay.

We have previously described the use of the CEAS detection for measurements in microtitre plates [18]. We now demonstrate the first use of LED-BBCEAS to absorption measurements for immunoassay in microtiter plates. Absorbance based microplate readers are one of the most commonly used instruments for bioassays. Their importance in clinical investigations is significant, however, the use of high cost analytes and antibodies make the consumable cost of certain bioassays expensive. The potential benefits of increasing the sensitivity of colorimetric detection include making the sensitivity of colorimetric bioassays comparable to fluorometric bioassays and also a reduction in the quantity and cost of expensive reagents needed to make a measurement for colorimetric bioassays where the existing sensitivity is sufficient.

EXPERIMENTAL SECTION

The optical cavity. Figure 1 shows a schematic of the experimental setup used. The optical cavity was constructed such that the linear cavity transmission axis and beam propagation direction was in the vertical plane to allow integration with the microplate reader which needed to move in the horizontal plane. The light source was a 1W Luxeon O Star white LED (Philips Lumileds Lighting Company, USA) which output ~50 mW in the range ~400-700 nm. The divergent output was collimated using a series of lenses and irises such that a 2 mW, nearly collimated beam of ~4 mm diameter was impingent on the first cavity mirror. The optical cavity was formed by two identical 25 mm diameter high reflectivity (R ≥ 0.99), concave mirrors (radius of curvature of = –100 mm, Layertec, Germany), which covered the range 420 nm - 640 nm and were separated by ~100 mm. The custom built microplate reader consisted of a motorised XY stage (Thorlabs MAX202, UK) controlled by a stepper motor controller unit (Thorlabs BSC103, UK) and associated personal computer (PC) based control software. The stage was able to move 105 mm in the x direction and 70 mm in the y direction with 10 μm accuracy. The microplate reader was placed between the cavity mirrors using a custom built lockable mount based on 4 translating post holders, which allowed fine adjustment of the tilt relative to the cavity mirrors.
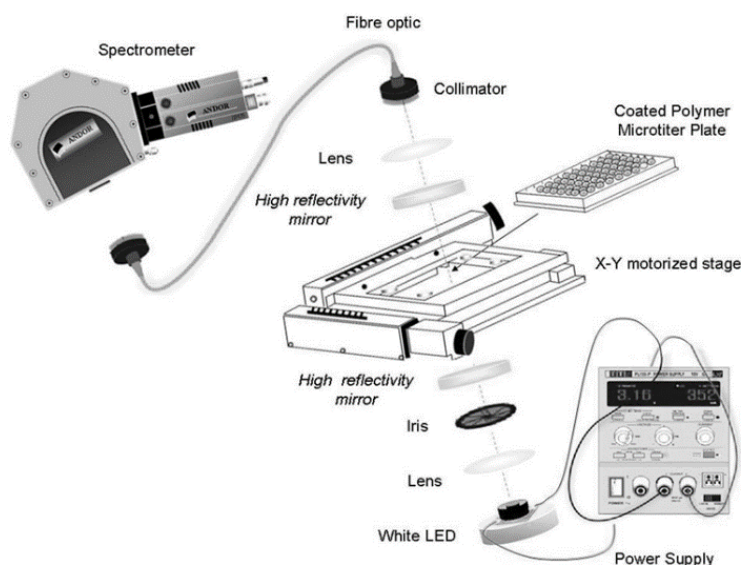

Figure 1. The schematic of the LED-BBCEAS experimental setup with an integrated custom built microplate reader.

During the course of experiments, three different types of 96 well microtiter plates were used to make measurements on liquid samples. Experiments were performed on either (i) glass bottomed (Thermo Scientific, UK, 12 mm pathlength and 370 μL well capacity) (ii) polystyrene bottomed microtiter plates (Microtest Ltd, UK, 11 mm pathlength and 360 μL well capacity) or (iii) protein coated polystyrene microtiter plates (IDS Ltd, UK, 11 mm pathlength and 360 μL well capacity) provided with the Osteocalcin ELISA.

The light exiting the cavity was focused by a 5 cm focal length lens onto the input of a 2 m long, 600 μm diameter fibre optic cable (Thorlabs M29L02, UK). The light leaving the fibre was focused by a

fibre optic collimator (Thorlabs F240-SMA, UK) onto the 100 μm entrance slit of the detection spectrometer. This consisted of an Andor Shamrock SR163 spectrograph coupled to a thermoelectrically cooled Andor iDus DV420-OE CCD camera, which operated over the range ~420 nm - 550 nm with ~1 nm resolution when used with a 1200 lines/mm grating. The spectrometer and recording of spectra was controlled through the software program SOLIS (Andor, UK) which ran on a PC which was connected to the CCD camera via a USB connection. Comparative conventional single pass microtiter plate measurements were made using a BioTek, Synergy HT Multi-Mode Microplate Reader (BioTek, USA) which had a stated minimum detectable change in absorbance of 1×10^{-3}.

Experimental methodology. Previous studies have shown that the absorption in a gas-phase CEAS experiment can be expressed by [19]:

$$\left(\frac{I_0(\lambda)}{I(\lambda)}\right)_{cavity} = 1 + \frac{2.303 \, \varepsilon_\lambda \, C \, l}{(1-R(\lambda))} \tag{1}$$

where, $I_0(\lambda)$ and $I(\lambda)$ are the measured transmitted intensities with and without the absorber in the cavity, l is the base path length through the sample in the cavity in cm, $R(\lambda)$ is the average wavelength dependent mirror reflectivity, ε_λ is the wavelength dependent extinction coefficient in ng^{-1} mL cm^{-1}, and C is the concentration of the sample in ng mL^{-1}. This expression, which is valid for all reasonable absorptions, shows that in a cavity experiment, $I_0(\lambda)/I(\lambda)$ is linearly proportional to the concentration of the analyte. It can be seen from Eqn.1 that the enhancement offered by a cavity experiment over a single pass experiment is due to the term $\frac{1}{(1-R(\lambda))}$. If this is set to be the wavelength dependent cavity enhancement factor (*CEF*), then the expression can be rearranged in terms of *CEF* [8]:

$$CEF(\lambda) = \frac{\left(\frac{I_0(\lambda)}{I(\lambda)}-1\right)_{cavity}}{2.303 \, \varepsilon_\lambda Cl} \tag{2}$$

Therefore, the *CEF* can be calculated at a given cavity absorption wavelength and concentration if the extinction coefficient of the analyte at a given wavelength ε_λ and the base path length of measurement are known, or if the cavity absorption and single pass absorbance (denominator term in Eqn.2) for the same sample is known. The *CEF* values can be averaged over several readings to obtain a more representative value. For measurements where the plot of cavity absorption against concentration was not expected to be linear, such as immunoassay standard curves, this was the approach taken. Alternatively if $\left(\frac{I_0(\lambda)}{I(\lambda)} - 1\right)_{cavity}$ is plotted versus concentration and the gradient of the linear plot divided by $2.303\varepsilon_\lambda l$, then a value of the *CEF* at a given wavelength and averaged over a range of concentrations is obtained. In this case of a linear relationship between cavity absorption and concentration a linear regression is fitted and the gradient obtained by a least squares method. The standard deviation in the measurement of the gradient can also be used to calculate the standard deviation in the *CEF* value. Although for gas-phase cavity measurements the $CEF(\lambda) = \frac{1}{(1-R(\lambda))}$ and thus can be used to determine the mirror reflectivity at a given wavelength, for the present liquid-phase measurements in a microtiter plate, the *CEF* value contains significant contributions from both solvent

4

and microtiter plate related scattering and absorption losses and thus is a measure of the total cavity loss. i.e.

$$CEF(\lambda) = \frac{1}{L_{total}(\lambda)}, \text{ where } L_{total}(\lambda) = \left[(1 - R(\lambda)) + L_{scat+abs}(\lambda)\right] \quad (3)$$

where $L_{total}(\lambda)$ is the per pass total cavity loss at a given wavelength and $L_{scat+abs}(\lambda)$ is the per pass scattering and absorption loss from the microtiter plate and solvent at a given wavelength.

The *CEF* value can be used to calculate the effective path length of measurement at a given wavelength ($l_{eff} = l \times CEF$) where l is the base path length. The effective path length is used in the calculation of the sensitivity of the measurement which is defined in terms of the minimum detectable change in the absorption coefficient α_{min} (also known as noise-equivalent absorption coefficient [19]). This is given by the expression:

$$\alpha_{min} = \frac{2.303 \, \Delta ABS_{min}}{l_{eff}} \quad (4)$$

where ΔABS_{min} is the minimum detectable absorbance change in the cavity absorption spectrum. This was determined by recording two successive I_0 spectra for a blank solution and calculating an absorbance spectrum by treating one of the spectra as the I spectrum. Ideally this 'blank' spectrum should consist of a flat line centered around an absorbance of zero. ΔABS_{min} could be calculated from this spectrum by measuring the standard deviation in absorbance around the wavelength of measurement which was usually the wavelength of peak cavity absorption.

The value of α_{min} could also be used to calculate the limit of detection (LOD) of an analyte which is defined as the smallest amount that can be reliably measured [15]. It was calculated from the expression:

$$LOD = \frac{3\alpha_{min}}{2.303\varepsilon_\lambda} \quad (5)$$

To allow a fairer comparison of the sensitivity of an experiment, the ΔABS_{min} values were normalised to one second of measurement by taking the total acquisition time in seconds (τ) into account by using the following expression:

$$\Delta ABS_{min}(t) = \Delta ABS_{min} \times \sqrt{\tau} \quad (6)$$

The time normalised $\alpha_{min}(t)$ value with units of cm^{-1} Hz$^{-1/2}$ for each measurement was given as:

$$\alpha_{min}(t) = \frac{2.303 \, \Delta ABS_{min}(t)}{l_{eff}} \quad (7)$$

Optimisation and alignment of the setup. The BBCEAS measurements in a microtiter plate introduced some new experimental challenges. Initially, the alignment of the empty cavity was

5

optimised by iterative adjustment of the kinematic controls on the top and bottom cavity mirror mounts, such as to maximise the output reaching the detector. This procedure was repeated when an empty microtiter plate was introduced into the cavity by the adjustment of the 4 lockable mounts relative to the cavity mirrors. The insertion of the microtiter plate led to a decrease in output intensity as a result of additional scattering and absorption losses. The glass bottomed microtiter plates, introduced a loss of ~20% compared to the ~50 - 70% loss of the lower optical quality polystyrene microtiter plates. The addition of phosphate buffer solution (PBS) as a blank solution for measurements, introduced a further cavity loss of ~10%. It was noticed that the total cavity loss (as measured by the intensity reaching the detector) was sensitive to the level of liquid in the well. The losses were high at levels below full well capacity, rapidly decreased as full well capacity was approached and then increased again as full well capacity was exceeded. On closer examination, the loss appeared to be related to the shape of the liquid/air interface. At levels less than full well capacity the shape of the meniscus was concave and resulted in higher interface scattering losses. As the level approached full well capacity the meniscus flattened leading to a substantial reduction in interface scattering losses. When the full well capacity was slightly exceeded the shape of the meniscus became convex, again leading to increased interface scattering losses. Consequently, to minimise interface losses, careful adjustment of the liquid level in the well was made using a syringe to optimise both the liquid level and shape of the interface. This was achieved through maximising the intensity reaching the detector.

Colorimetric reaction. Preliminary experiments to optimise the experimental setup were performed on a colorimetric reaction involving the enzyme linked conjugate Streptavidin-Horseradish Peroxidase (STREP-HRP), as this reaction was also used as part of the subsequent osteocalcin ELISA assay. The reaction was performed in both glass and polymer bottomed microtiter plates to determine the relative optical losses of the two types of microtiter plates.

A 25 µg mL^{-1} STREP-HRP conjugate was used as a stock solution to prepare serial dilutions of the enzyme linked protein in the range from 0.1 ng mL^{-1} to 0.8 ng mL^{-1}. The colorimetric reaction was carried out in clear 7.0 mL sterile plastic containers (Bijou PP, SLS Ltd) under dark conditions. 3,3',5,5'-tetramethylbenzidine (TMB) was used as a non-carcinogenic substrate solution and was pipetted into each STREP-HRP solution in a 1:10 ratio (100 µL of STREP-HRP and 1 mL of TMB). After 15 minutes incubation time the chromogenic substrate was enzymatically oxidised to a blue coloured product. Upon addition of 1mL of sulphuric acid to each vial a yellow colour change took place and samples were immediately transferred into appropriate microplate wells for absorption measurement at 450 nm in the cavity. Phosphate buffer solution (PBS) at a pH 7.4 was used as a blank solution for each of the samples. The absorption at 450 nm directly reflected the quantity of streptavidin present in each sample. Cavity absorption measurements were repeated three times at each concentration in the range 0.1 ng mL^{-1} to 0.8 ng mL^{-1} and the results were compared with single pass absorption measurements in a 1 cm quartz cuvette, using a conventional UV-Visible double beam spectrometer (Jasco V-630).

Sandwich ELISA. A commercially available ELISA kit (N-MID Osteocalcin, IDS diagnostics) was chosen for the application of BBCEAS. The assay is a well-known immunological diagnostic test widely used in metabolic bone disorder clinical research. The test is designed to detect and quantify osteocalcin in human serum and plasma. Osteocalcin is a non-collagenous calcium binding protein mainly produced by osteoblasts. After synthesis, it is delivered to bone matrix and also partially released into the circulation system. As it originates from bone, the amount of osteocalcin present in serum directly reflects bone formation activity. Indication of osteoblast activity is a valuable aid in identifying individuals at a risk of developing osteoporosis or conditions that are associated with both high and low bone turnover respectively, such as growth hormone deficiency or hyper- and hypo-parathyroidism. The

method was based on a sandwich ELISA, using a biotinylated monoclonal antibody as a capture antibody and an HRP-labelled monoclonal antibody as a detection antibody. Detection is accomplished by measuring the activity of the peroxidase enzyme with a chromogenic substrate. The absorption of the resulting coloured product is directly proportional to the concentration of osteocalcin present in the sample.

The ELISA kit contained a 96 well polystyrene microtiter plate. The bottom of each well was coated with a layer of streptavidin. Each subunit of the tetrameric protein can strongly bind four molecules of biotin. During the assay the strong bond between the two compounds is utilized to attach biotin-labelled osteocalcin antibody to the streptavidin coated plate.

Assay procedure. The complete ELISA procedure was carried out at room temperature (~22°C). The antibody solution was prepared by adding 10 mL of the diluted conjugated solution to both the peroxidase, and biotinylated antibody and then mixing equal volumes of the two solutions together. The ELISA kit contained synthetic human osteocalcin standards (CAL 1-5) which were reconstituted with 500 µL of distilled water, resulting in solutions of concentration 3.7 ng mL^{-1} to 61.6 ng mL^{-1}. CAL 0 was a blank solution which contained PBS, protein stabilizer and preservatives.

Figure 2 shows a schematic of the ELISA procedure. Immuno strips incubation required 20 µL of the CAL 0-5 standards to be pipetted into appropriate wells (a), followed by addition of 150 µL of the mixed antibody solution (b). The strips were incubated for 120±5 minutes without any mixing under dark conditions. The wells were washed 5 times with approximately 300 µL of washing buffer solution to remove excess antibody solution (c). For the final stage, 250 µL of chromogenic TMB substrate solution was pipetted into each well except the one containing the PBS blank solution (d). After 15±2 min incubation in the dark, TMB was oxidized by the enzyme HRP attached to the detection antibody to yield a blue colour. The reaction was stopped by adding 250 µL of H$_2$SO$_4$ stopping solution to each well, resulting in a final yellow colour (e). The total volume of liquid added slightly exceeded the total capacity of the well (360 µL) leading to a convex bulge on top of the well. A flat surface layer was ensured to minimise interface losses as described previously (f). Comparison was made by determining the osteocalcin ELISA standard calibration curve using a conventional microplate reader (BioTek, Synergy HT) to make absorbance measurements at 450 nm.
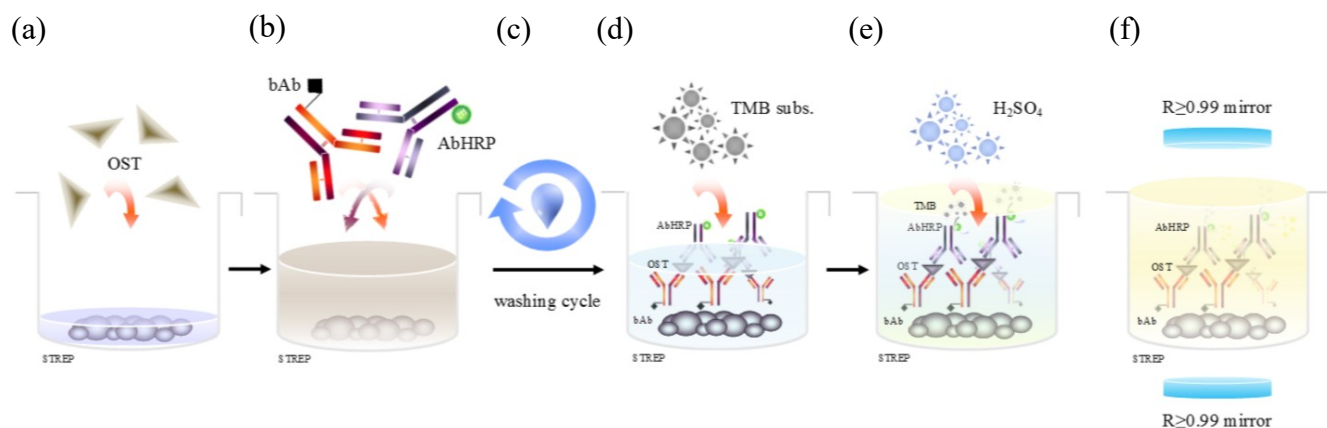

Figure 2. Osteocalcin assay procedure: (a) CAL 0-5 standards, (b) mixed antibody solution, (c) removal of excess antibodies, (d) TMB substrate solution, (e) H$_2$SO$_4$ stopping solution, (f) Cavity enhanced measurement.

7

RESULTS AND DISCUSSION

Colorimetric reactions. The colorimetric reaction between STREP-HRP and TMB was studied in both polystyrene and glass bottomed microtiter plates. Figure 3 shows (a) a representative cavity absorption spectrum of STREP-HRP in a glass bottomed plate in the range 400 nm - 520 nm and at a concentration of 0.2 ng mL^{-1} and (b) a cavity absorption plot in a polymer plate at concentrations ranging from 0.1 ng mL^{-1} to 0.8 ng mL^{-1}. Table 1 lists the figures of merit for the measurements along with those for the osteocalcin ELISA measurements. It can be seen that the *CEF* value at 450 nm for the measurements in the glass bottomed microtiter plates (55.6) is significantly higher than that in the polymer bottomed plates (33.8) as a result of the better optical quality which produces lower optical losses in the optical cavity. This also leads to lower ΔABS_{min} values as a higher intensity reaches the detector and as the noise is proportional to the square root of the intensity at the detector, for cases such as these which are essentially shot noise limited. This also contributes to lower $\alpha_{min}(t)$ and *LOD* values. However, the polymer bottomed microtiter plate results still produce a substantial improvement in both path length and sensitivity (42 fold, Table 1) when compared to a single pass measurement. This is important because current bio-analytical microtiter plate measurements are typically performed in polymer bottomed microtiter plates.

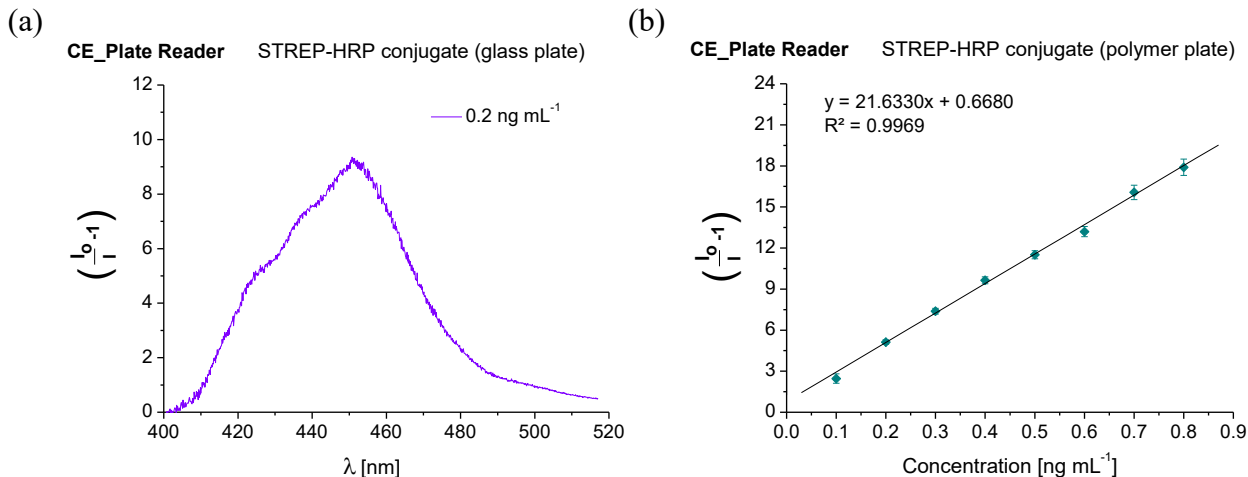(a)   (b)

Figure 3. (a) Representative cavity absorption spectrum of the STREP-HRP conjugate obtained in a glass bottomed microtiter plate. (b) Cavity absorption plot in a polymer bottomed microtiter plate.

Table 1. Summary of the results in terms of the assay plate, the base path length, the *CEF* value at 450 nm and the standard deviation of the measurement, the $\alpha_{min}(t)$ and the LOD of the analyte, and the minimum detectable change in absorbance noise $\Delta ABS_{min}(t)$ at 450 nm with R≥0.99 mirror set.

Technique	Sample	Microtiter plate	*l* /cm	*CEF*	$\Delta ABS_{min}(t)$	$\alpha_{min}(t)$ /cm^{-1} Hz$^{-1/2}$	LOD (ng mL^{-1})
CE-Plate Reader	STREP-HRP	Glass	1.2	55.6 ± 1.3	5.25×10^{-4}	1.81×10^{-5}	9.35×10^{-5}
CE-Plate Reader	STREP-HRP	Uncoated polymer	1.1	33.8 ± 0.8	8.02×10^{-4}	4.96×10^{-5}	2.56×10^{-4}
CE-Plate Reader	OST ELISA	Strep coated polymer	1.1	30.2 ± 4.6	7.45×10^{-4}	5.33×10^{-5}	2.75×10^{-4}
Standard Plate Reader		Polymer	1.1		1×10^{-3}	2.09×10^{-3}	

Osteocalcin ELISA. BBCEAS measurements were made on the calibration solutions from a commercial osteocalcin kit. These results were compared with measurements performed in a standard microplate reader to determine the *CEF* values at 450 nm using Eqn. 2 whilst other figures of merit are also listed in Table 1. Figure 4 shows (a) the cavity enhanced absorption plot of human osteocalcin standards (CAL 1-5) and the blank solution (CAL 0) as a function of concentration in the range 0 ng mL^{-1} to 61.6 ng mL^{-1} and (b) the single pass calibration curve using the standard microplate reader. Both plots show a characteristic sigmoidal curve due to cooperative binding between the antibody and antigen. The reduction in average number of passes (30.2) when compared to polymer bottomed plates for STREP-HRP (33.8) was most probably the result of the increasing effect of stray light in the spectrometer on the higher analyte concentrations (Table 2) which produced very large absorptions. This would be expected to lead to the measured absorption being lower than the true absorption and thus an underestimate of the calculated *CEF* value. Although the better optical quality of the ELISA microtiter plate produced lower optical losses in the optical cavity and resulted in lower $\Delta ABS_{min}(t)$, the lower *CEF* value contributed to higher $\alpha_{min}(t)$ and LOD values. The results obtained in the studied concentration range were significant as they showed the ability of the system to measure higher analyte concentrations and thus broaden its applicability.
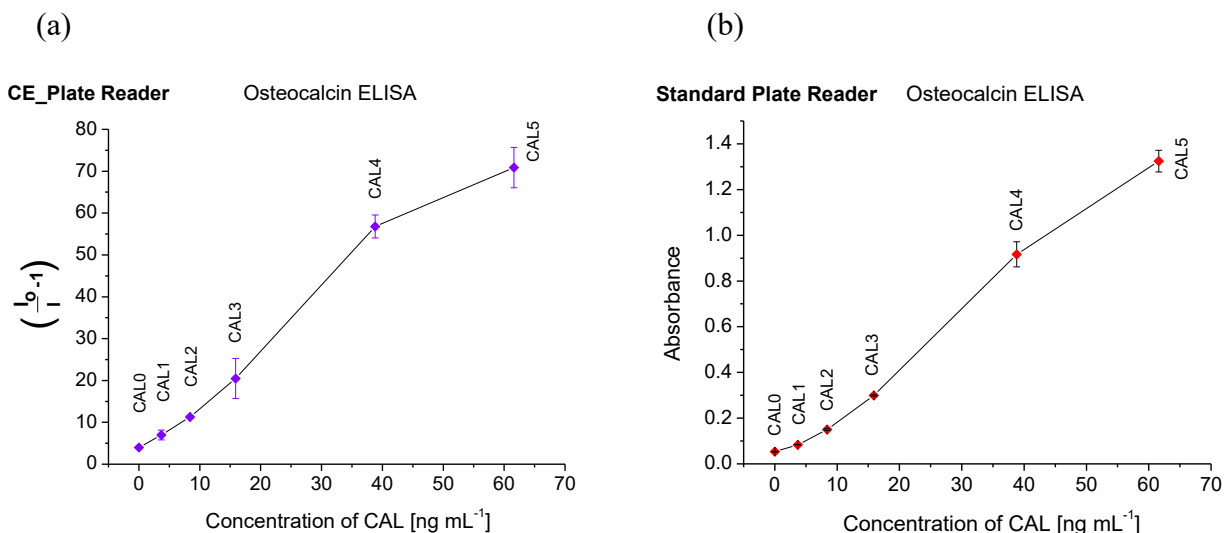
(a)   (b)

Figure 4. The absorption versus concentration plot of human osteocalcin ELISA in the range 0 ng mL^{-1} to 61.6 ng mL^{-1}. The error bars represent the standard deviation of the measurements. (a) The measurement in the cavity enhanced microplate reader. (b) The corresponding calibration curve obtained in the standard microplate reader.

Table 2. The value of the *CEF* at 450 nm obtained for individual human osteocalcin standards (CAL 1-5) in the concentration range 0 ng mL^{-1} to 61.6 ng mL^{-1}. The average *CEF* and the standard deviation of the measurement is also listed.

CE-Plate Reader OST ELISA		
OST standards	**Conc./ng mL^{-1}**	***CEF***
CAL 0	0.00	32.5
CAL 1	3.70	36.2
CAL 2	8.40	32.6
CAL 3	15.9	29.7
CAL 4	38.8	26.9
CAL 5	61.6	23.2
	Average *CEF*	**30.2 ± 4.6**

Comparison with previous studies. Table 3 compares the best figures of merits from our study with some of the previously reported liquid-phase cavity enhanced studies in cells of 1 cm base path length.

When comparing the sensitivity of our measurements with measurements in a conventional microplate reader our results (Table 1) are between 39 and 115 fold more sensitive, showing that a very significant increase in sensitivity can be achieved without much additional cost or experimental complexity. The increase in sensitivity also means that colorimetric measurements can begin to approach the sensitivity of fluorometric measurements.

Table 3. Comparison between this study and the data available from previous liquid-phase cavity studies as a function of technique, the mirror reflectivity, the light source, the cell used, the wavelength of measurement, the base path length and the lowest value of α_{min}, the minimum LOD and the extinction coefficient for the analyte in question.

Study	Technique	R≥	Light source	Cell	λ/nm	l/cm	α_{min}/cm^{-1}	LOD/ng mL^{-1}	ε/ng^{-1} mL cm^{-1}
STREP-HRP	CE-Plate Reader	0.99	white LED	glass plate	450	1.2	1.81×10^{-5}	9.35×10^{-5}	2.52×10^{-1}
OST ELISA	CE-Plate Reader	0.99	white LED	polymer plate	450	1.1	5.33×10^{-5}	2.75×10^{-4}	2.52×10^{-1}
Qu et al. [20]	BBCEAS	0.99	LED	cuvette	527	1.0	6.5×10^{-5}	4.1×10^{-1}	2.1×10^{-4}
Seetohul et al. [17]	BBCEAS	0.99	LED	HPLC cell	556	1.0	1.9×10^{-5}	1.0	1.9×10^{-4}
Fiedler et al. [21]	BBCEAS	0.99	lamp	cuvette	607	1.0	2.0×10^{-5}	-	-
Xu et al. [22]	CRDS	0.9997	pulsed laser	cuvette	607	1.0	1.0×10^{-5}	-	-
van der Sneppen et al. [23]	CRDS	0.9995	Nd:YAG laser	cuvette	355	1.0	3.0×10^{-5}	8.4	4.7×10^{-5}
van der Sneppen et al. [23]	CRDS	0.9991	Nd:YAG laser	cuvette	273	1.0	1.0×10^{-3}	1.3×10^{2}	-

Most of the previous liquid-phase cavity studies in 1 cm base path length cell have been performed using generally more complex and expensive experimental setups and also higher reflectivity mirrors. The first study by Xu et al. [22] CRDS on the C-H stretching fifth vibrational overtones of benzene and reported a value of α_{min} of 1.0×10^{-5} cm^{-1}. HPLC-CRDS measurements by van der Sneppen et al. [23] at 355 nm and 273 nm had lower sensitivity as a result of the decreased performance of the high reflectivity mirrors in the deep UV region. Fielder et al. [21] made the first demonstration of liquid- phase BBCEAS whilst Seetohul et al. [17] reported the first HPLC-BBCEAS measurements. Qu et al. [20] made BBCEAS measurements using a simple low cost webcam based spectrometer. The sensitivity of the measurements in the present study compares favorably with all the previous studies showing that similar levels of sensitivity can be achieved in microtiter plates as in cuvettes. Table 3 lists the best LODs obtained in this study and the comparison with the LODs, where available, of previous liquid-phase cavity studies. The value of the LOD is affected both by the calculated value of α_{min} and the absorptivity for the particular analyte. As would be expected the glass bottomed microtiter plate gave the lowest LOD for the strong absorber STREP-HRP. The increased losses in polymer bottomed plates led to higher α_{min} and LOD values. The LODs in this study compare favorably with previous studies taking into the account the differences in the extinction coefficients of the analytes studied.

We have shown here a successful application of LED-BBCEAS detection for immunoassay and colorimetric reactions in a microplate reader. The LED-BBCEAS approach has been shown to provide around a 100 fold increase in sensitivity over conventional microplate readers which can lead to lower LODs and/or reduced consumption of reagents within the assay and allow colorimetric detection to approach the sensitivity of fluorometric detection.

Further work. Although our LED-BBCEAS system showed significant improvement over conventional microtiter plate readers and the performance of the technique compares favourably with previous liquid-phase cavity studies, the current sensitivity could be improved by a number of modifications. Losses related to the shape of the liquid/air interface can be further reduced by use of automated liquid dispensing to measure out accurately the exact amount of samples needed to fill the well and/or use of a lid to cover the surface of the microtiter plate to flatten the meniscus. It should be noted that the use of higher reflectivity cavity mirrors to increase the number of passes through the cavity would be ineffective due to the dominant optical losses from the polymer microtiter plate. Higher sensitivity could be achieved by using high quality glass bottomed microtiter plates but this would require appropriate coatings specific for antigen-antibody binding. A number of further improvements could be made, including fibre coupling the light exiting the cavity on to the thermoelectrically cooled CCD detector for higher light throughput and improved signal to noise.

CONCLUSION

We describe the first report on the detailed use of cavity enhanced detection for immunoassay measurements in microplate readers. A vertical $R \geq 0.99$ optical cavity using a broadband LED light source and a CCD spectrograph was integrated with a custom built microplate reader to perform colorimetric bio-analytical measurements. The major advantage over conventional microplate readers is provided by the increased sensitivity of the setup which has the benefit of lower detection limits in conjunction with reducing the consumable cost of currently expensive bioassays. Experiments performed on a commercially available osteocalcin ELISA showed a 39 fold improvement in sensitivity when compared to measurements in a standard microplate reader, whilst measurements on the STREP-HRP reaction showed up to a 115 fold increase in sensitivity. This makes colorimetric detection approach the sensitivity of fluorometric detection in microplate readers. In comparison with previous liquid-phase CEAS and CRDS studies in 1 cm cuvettes, the lowest α_{min} values from our studies were found to offer similar sensitivities, using microtiter plates with generally higher optical losses. Further

improvements can be made in light coupling as well as developing a more compact and robust integrated cavity enhanced detection system.

Acknowledgements

REFERENCES

1   Taipa, M. Â. *Comb.Chem.High Throughput Screen.* **2008**, *11*, 325-335.

2   Armstrong, S.; Miao, Z. -.; Rowell, F. J.; Ali, Z. *Anal.Chim.Acta.* **2001**, *444*, 79-86.

3   Rincón, V.; Corredor, A.; Martínez-Gutíerrez, M.; Castellanos, J. E. *J.Virol.Methods.* **2005**, *127*, 33-39.

4   O'Keefe, A.; Deacon, D. A. G. *Rev.Sci.Instrum.* **1988**, *59*, 2544-2551.

5   Engeln, R.; Berden, G.; Peeters, R.; Meijer, G. *Rev.Sci.Instrum.* **1998**, *69*, 3763-3769.

6   Fiedler, S. E.; Hese, A.; Ruth, A. A. *Chemical Physics Letters.* **2003**, *371*, 284-294.

7   Ball, S. M.; Langridge, J. M.; Jones, R. L. *Chemical Physics Letters.* **2004**, *398*, 68-74.

8   Van Der Sneppen, L.; Hancock, G.; Kaminski, C.; Laurila, T.; MacKenzie, S. R.; Neil, S. R. T.; Peverall, R.; Ritchie, G. A. D.; Schnippering, M.; Unwin, P. R. *Analyst.* **2010**, *135*, 133-139.

9   Rushworth, C.; Vallance, C. *Proceedings of SPIE - The International Society for Optical Engineering.* **2010**, *7838*

10   Kiwanuka, S. -.; Laurila, T.; Kaminski, C. F. *Anal.Chem.* **2010**, *82*, 7498-7501.

11   Neil, S. R. T.; Rushworth, C. M.; Vallance, C.; MacKenzie, S. R. *Lab on a Chip - Miniaturisation for Chemistry and Biology.* **2011**, *11*, 3953-3955.

12   James, D.; Oag, B.; Rushworth, C. M.; Lee, J. W. L.; Davies, J.; Cabral, J. T.; Vallance, C. *Rsc Advances.* **2012**, *2*, 5376-5384.

13   Kiwanuka, S. -.; Laurila, T. K.; Frank, J. H.; Esposito, A.; Blomberg Von Der Geest, K.; Pancheri, L.; Stoppa, D.; Kaminski, C. F. *Anal.Chem.* **2012**, *84*, 5489-5493.

14   Rushworth, C. M.; Jones, G.; Fischlechner, M.; Walton, E.; Morgan, H. *Lab Chip Miniaturisation Chem.Biol.* **2015**, *15*, 711-717.

15   Islam, M.; Seetohul, L. N.; Ali, Z. *Appl.Spectrosc.* **2007**, *61*, 649-658.

16   Seetohul, L. N.; Ali, Z.; Islam, M. *Analyst.* **2009**, *134*, 1887-1895.

17   Seetohul, L. N.; Ali, Z.; Islam, M. *Anal.Chem.* **2009**, *81*, 4106-4112.

18   Ali, Z.; Seetohul, L. N.; Auger, V.; Islam, M.; Scott, S. M. *Microfluidic device with CEAS detection.* **2008**, *US 8,325,342 B2*

19   Mazurenka, M.; Orr-Ewing, A. J.; Peverall, R.; Ritchie, G. A. D. *Annual Reports on the Progress of Chemistry - Section C.* **2005**, *101*, 100-142.

20   Qu, Z.; Engstrom, J.; Wong, D.; Islam, M.; Kaminski, C. F. *Analyst.* **2013**, *138*, 6372-6379.

21   Fiedler, S. E.; Hese, A.; Ruth, A. A. *Rev.Sci.Instrum.* **2005**, *76*, 023107-1-023107-7.

22   Xu, S.; Sha, G.; Xie, J. *Rev.Sci.Instrum.* **2002**, *73*, 255.

23   van der Sneppen, L.; Ariese, F.; Gooijer, C.; Ubachs, W. *Journal of Chromatography A.* **2007**, *1148*, 184-188.

Table of contents graphic